IMPINGEMENT OF A DROPLET ONTO A DRY WALL: A NUMERICAL INVESTIGATION

N. Nikolopoulos, and G. Bergeles[1]
Department Mechanical Engineering
Nat. Technical University of Athens
15740 Zografos, Greece

The impingement of a drop on a dry solid surface has been investigated. For the numerical simulation of the process, the Volume of Fluid (V.O.F) methodology is used coupled with a numerical Navier-Stokes solver. The fluids are modeled as a continuum with a jump in the fluid properties at the interface. Each fluid is marked with a distinguishable value of indicator function, while the interface is the region, where this function, experiences a steep change. Details of the flow fields inside and outside the droplet are calculated. The computational results of the cases examined agree well during the advancing phase with corresponding numerical-experimental data, found in the literature. It is proven however that important role in the development of the impinging process plays the ability of the liquid to wet the surface (wettability) as it is expressed by the dynamic contact angles. Particularly it seems that the dynamic contact angle during the receding phase is a function of the velocity of the receding droplet front.

1. Introduction

The study of the impact of a single droplet on a solid dry surface is of importance in many industrial applications, such as spray cooling, inkjet printing or fuel injecting. The dynamics of the impact of a single droplet onto a solid wall depend not only on the properties of the impinging droplet (primary), but also on the solid surface properties.

The droplet-solid wetting properties are expressed arithmetically through the value of the advancing dynamic contact angle (advancing phase) and the receding dynamic contact angle (receding phase). The contact angle is defined geometrically as the angle formed by a liquid at the three phase boundary where a liquid, gas and solid intersect. Low values of ? indicate that the liquid spreads, or wets well the solid surface, while high values indicate poor wetting. If ? is greater than 90, the system liquid-solid is said to be non-wetting. A zero contact angle represents the case of a complete wetting of the surface by the liquid phase. The impact of the droplet onto the solid wall, depending on the initial conditions, can lead to droplet deposition, droplet splashing, or to droplet rebound. Each of these three cases are followed by other secondary effects. A detailed description of those cases is given by R.Rioboo [2]; during deposition, the droplet is only deformed and stays on the surface; Cossali et al. [1] present a correlation between the critical number ($K=Oh^{1.25}$ Re) K_{crit}, separating the two main phenomena that occur after the initial impact, i.e. deposition or splashing, and the dimensionless roughness. This critical number was given as: $K_{crit} = 649 + 3.76 \cdot R_{nd}^{-0.63}$

[1] Author to whom correspondence should be addressed
e-mail:bergeles@fluid.mech.ntua.gr

In this equation R_{nd} is the dimensionless roughness of the solid surface. Mundo, Sommerfeld and Tropea [3] studied the splash of drops using various liquids, impact velocities, droplet diameters, roughness amplitudes and angles of impact in order to find a splash / deposition and a deposition / break-up limit. The critical value of K, K_{cr}, below which deposition occurs and above which splash occurs, was shown to be also a function of mean roughness amplitude, as shown by Cossali et al. As the roughness amplitude increases, the critical value of K reaches an asymptotic value of K_{cr} = 57.7 or K'_{cr} = 657, which is written as a function of Weber (We) and Ohnesorge (Oh) numbers ($K'_{cr}= K_{cr}^{8/5}$). This value (K'_{cr} = 657) is valid only for dimensional roughness of order of magnitude of droplet diameter.

2. *The Mathematical problem*

The flow induced by a liquid droplet impinging onto a wall is considered here as two dimensional axisymmetric, incompressible and laminar; the two phase flow (phase 2 is the liquid phase, i.e the droplet, phase 1 is the surrounding gas) is represented by the Navier-Stokes equations and the continuity equation with extra terms which take into account the forces due to surface tension effects and gravity. The values of density and viscosity for each phase are constant, and in the transitional area between the two phases (interface) there is a linear interpolation of the different properties of fluids from both sides of the interface.

For identifying each phase separately a volume fraction, named a, is introduced following the Volume of Fluid Method (VOF) of Hirt and Nichols [4]. In the V.O.F method the volume fraction a is defined as:

$$a = \frac{\text{Volume of fluid 1}}{\textit{Total} \text{ volume of the control volume}}$$

The value of density and viscosity are calculated as a function of a, using linear interpolation between the values of the two phases:

$$? = a?_1 + (1-a)?_2$$
$$\mu = a\mu_1 + (1-a)\mu_2$$

where, ***a****-function* is equal to:

$$a(x,t) = \begin{cases} 1, & \text{for the point (x, t) inside fluid 1} \\ 0, & \text{for the point (x, t) inside fluid 2} \\ 0 < a < 1, & \text{for the point (x, t) inside the transitional area between the two phases} \end{cases}$$

The momentum equations expressing both phases are written in the form

$$\frac{\partial(?\vec{u})}{\partial t} + \nabla \cdot (?\vec{u} \otimes \vec{u} - \vec{T}) = ?\vec{g} + \vec{f}_s \qquad (1)$$

where T is the stress tensor. The value of f_s is equal to: $f_s = s \cdot ? \cdot (\nabla a)$, where s is the numerical value of the surface tension (for immiscible fluids the value is always positive) and ? is the curvature of the interface region.

The curvature of the interface may therefore be expressed in terms of the divergence of the unit normal vector to the interface, as follows:

$$k = -\nabla \cdot (\frac{\nabla a}{|\nabla a|}) \quad \text{and} \quad f_s = -s \cdot [\nabla \cdot (\frac{\nabla a}{|\nabla a|})](\nabla a)$$

Following Hirt and Nichols the location of the interface is calculated on the assumption that the material derivative of the VOF indicator a is zero:

$$\frac{\partial a}{\partial t} + u \cdot \nabla a = 0$$

The continuity equation, using the conservation of the VOF indicator a can be written:

$$\nabla \cdot u = 0 \qquad (2)$$

Using the above equation, the conservative form of the transport equation for a is therefore:

$$\frac{\partial a}{\partial t} + \nabla \cdot au = 0 \qquad (3)$$

3. *The numerical solution procedure*

Transport equations are solved numerically by the Finite Volume Method using a collocated grid arrangement; the descretisation of the convection terms is based on the BSOU method of Papadakis and Bergeles [5], a second order bounded upwind method, whilst the solution procedure follows the SIMPLE algorithm of Patankar and Spalding [6] with the modifications of Rhie and Chow [7] to avoid pressure velocity decoupling. Due to the steep gradients of the VOF indicator a which appear particularly in the region of the interfaces, the compressive high resolution differencing scheme CICSAM of Onno Ubbink [8] which restricts the transitional area of the two fluids within two cells was found necessary to be implemented in the transport equation of a, for a good resolution of the transitional region, as other descretisation schemes failed to capture the sharp and smooth interface between the two fluids. The time derivative was discretized using a second-order differencing scheme (Crank-Nicolson).

4. Numerical details

The main parameters of the impact of a single droplet onto a solid wall taken into account are droplet diameter D_o, initial impact velocity U_o surface tension s and dynamic contact angles, representing wettability i.e. advancing and receding. These variables are grouped in a set of dimensionless parameters: We, Bo and Re.

The flow domain is axisymmetric (along the x-axis gravity) and the liquid phase (droplet) is water, whilst the surrounding gas is air. So the real state of the droplet is represented if the results are rotated around the X – axis. The dimensions of the computational domain, are X_{total} =1.6 D_o and Y_{total} =3.2 D_o. The numerical grid consists of 33600 (160 X 210) cells and gave a grid independent solution for grids above of 27000 (150 X 180) cells. At the start of calculations the droplet is covered by 2495 cells.

5. Results and discussion

Two main cases, whose main parameters are shown in Table 1 have been investigated.

	Ro (mm)	Uo (m/sec)	Re	We	Bo	T_{cs} (deg)	T_{cr} (deg)
Case A	1.88	1.5	3010	58.4	0.478	60	22
Case B	1.86	1.58	3130	64.1	0.468	92	60

Table 1: Test cases examined

Spherical droplets of water collide with a flat surface of two different materials. In the first case (Case A) the flat surface is made of pyrex glass while in the second case (Case B) made of wax. The dynamic contact angles (advancing and receding) were determined from separate experiments in which the droplet was allowed to slide freely down an inclined test surface. These measurements have been done by J.Fukai et al [9]. For the simulation of these cases, constant values for the dynamic contact angles both in the spreading and recoiling stages, independent of the velocity of the contact line have been assumed. J.Fukai et al, stated that contact angles are almost constant, if the flow is not characterized by high capillary number (capillary phenomena).

J.Fukai et al. adopted a Lagrangian approach, simulating the motion of the deforming free surface solving the N-S equations. In contrast with the numerical model used by J.Fukai et al. for predicting such a phenomenon, the VOF methodology employed here solves not only for the liquid but also for the gas phase.

Gravity has probably little effect on the fluid dynamics of the impacting water droplets because the Bond number, which is the ratio of the gravitational force to surface tension force, is small. The advancing (T_{cs}) and receding (T_{cr}) contact angles are also listed in Table1. All numerical simulations for the two cases were carried out until non-dimensional time T= 60. The values of dynamic contact angles in Case B are greater than in Case A, which means that the surface made of wax is more wettable than the one made of pyrex. So water droplet spreads easier in Case A than in Case B.

This is verified from the figures 1 and 2, where the radius of the lamella is presented as a function of time, for both cases. In these figures experimental data, obtained from J.Fukai et

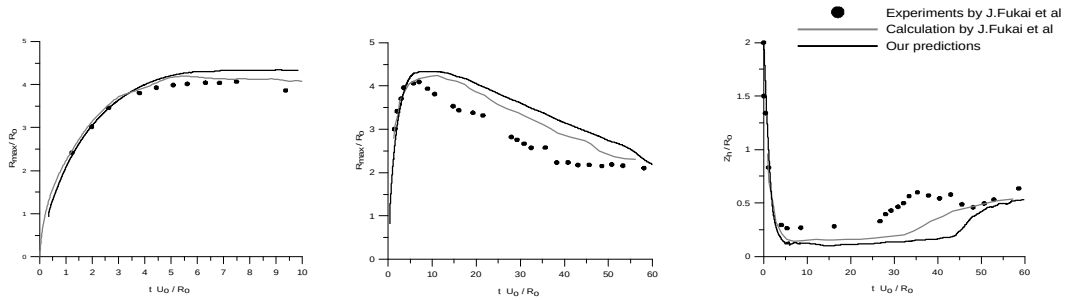

Figure 1: Maximum radius and height of spreading lamella versus time for Case A

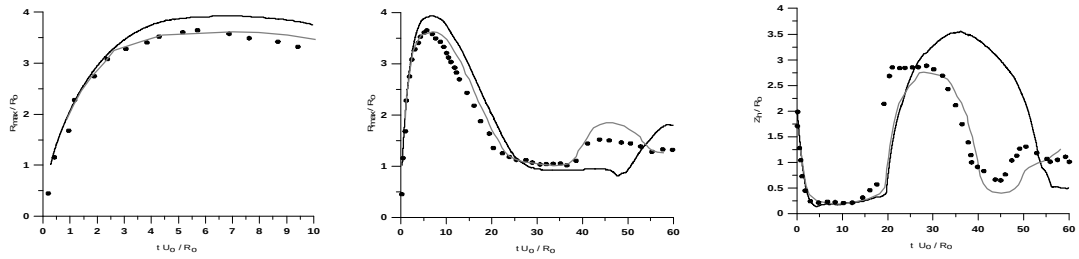

Figure 2: Maximum radius and height of spreading lamella versus time for Case B

al., are compared with our predictions and also to the predictions obtain by Fukai et al. using the Lagrangian approach. The predicted droplet spread is close to the experiments up to a non dimensional time of T=7.6, but for greater times there are discrepencies. Evidently the differencies are due to a type of hysterisis which appears during the transition of the lamella front from advancing to receding phase. It seems that there is dependence between the value of dynamic contact angles and the velocity of the rim of the lamella. In the literature models exist as that of Hoffmann [10], Blake [11] complemented by M.Marengo's [12] modification; the latter correlation is used in the present numerical code and the predicted results are slightly improved, especially during the receding phase (figure 3).

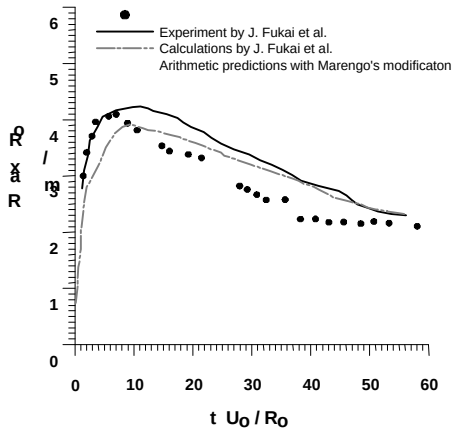

Figure 3: Maximum radius of spreading lamella versus time for Case A, applying Marengo's law

Figures 4 and 5 show in a sequence of frames, detailed evolution of the droplet spreading. Two main dynamic phases, the spreading and the recoiling one characterize the motion of the spreading lamella. At the first stages of impact, around the droplet a thin film (lamella) is

formed, which spreads outwards on the solid surface. During its spreading mass accumulates at the periphery of the droplet, forming a ring structure. This happens because forces of wettability in that region obstruct the free flow of lamella.The inward thickness of lamella is. The outward motion stops at about time T=10.0. The corresponding time for case B is T=6.0. This is the end of the spreading phase. One would expect that the recoiling phase would start

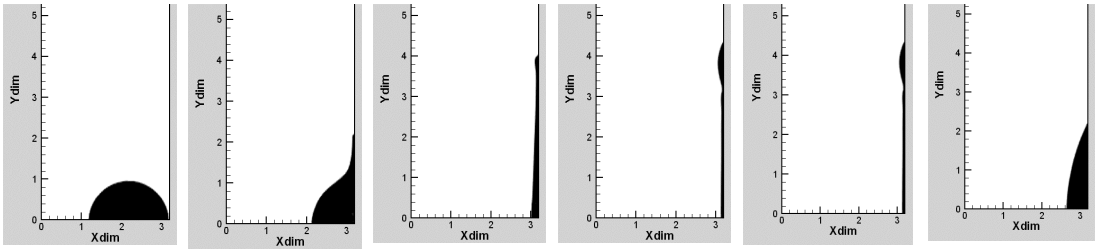

? =0.0 ? =1.0 ? =4.0 ? =10.0 ? =40.0 ? =60.0

Figure 4: Time evolution of Case A

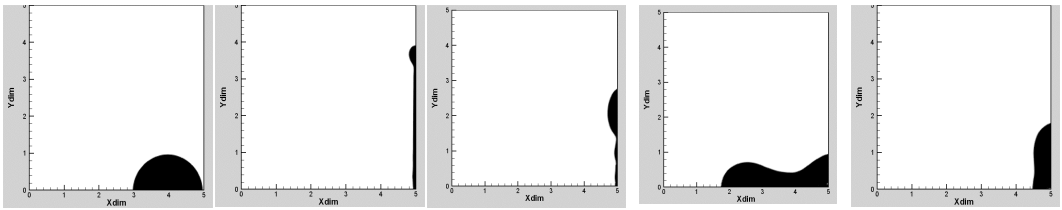

? =0.0 ? =6.0 ? =16.0 ? =42.0 ? =60.0

Figure 5: Time evolution of Case B

immediately after the end of the first phase. This doesn't happen because of the phenomenon of hysterisis.

From sequence of frames it is deduced that the contact line remains stationary till about time T=11.0 for case A. Afterwards the dynamic contact angle deceases and its value adjusts from the advancing to the receding one. This happens because liquid phase is moving through the bottom of the ring outward, and feeds the ring structure, while in the top of the ring, there is an inward movement. This combination of movements decreases step-by step the value of the dynamic contact angle. The droplet begins to recede, but the film thickness of the receding lamella continues to thin, accumulating fluid at the rim. This continues till time T=40.0. The corresponding time for case B is T=16.0. During the advancing phase, the initial kinetic energy of the droplet is dissipated; during the recoiling phase the droplet recedes under the effect of surface tension. That is why the receding phase outlasts in comparison with the spreading phase. At the end of the receding phase in case A and especially in case B, the droplet oscillates for some time, till it reaches its equilibrium state. This happens at about T=60.0 in both cases. Especially in case B where the receding contact angle is greater than in case A, and the receding velocity is higher the effect of gravity is rather important. For example this oscillation in case A lasts from time T=50.0 till time T=60.0, whilst in case B is almost double. Figures 6 and 7 indicate the velocity vector distribution and the pressure distribution in both phases, with time. It is of interest to notice the continuity of the velocity field through the gas liquid interface, as also the well defined liquid gas interfaces, an

indication of the non-diffusive character of the CICSAM discretisation scheme. It is of interest also to note that both the maximum non- dimensional pressure and air jetting velocity are about equal in cases A and B, indicating the similarity of the impinging process at the initial stages of droplet impact.

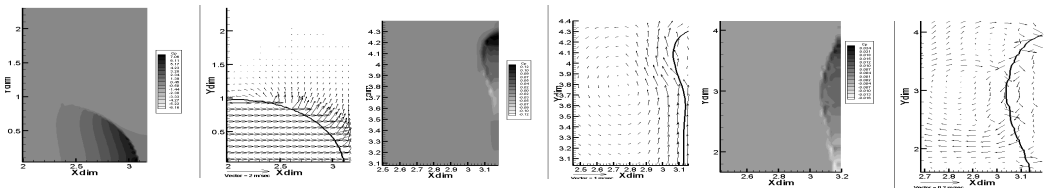

T=0.0 T=6.0 T=20.0

Figure 6: Velocity and Pressure field of Case A

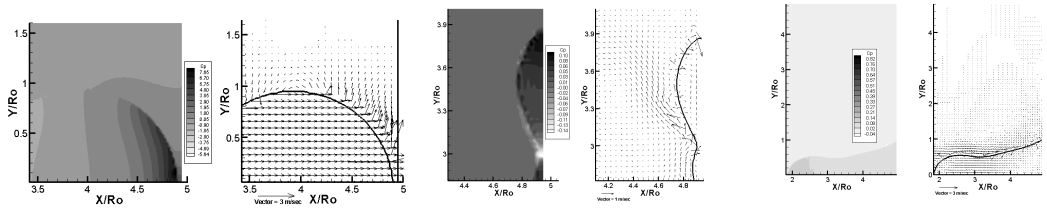

T=0.0 T=8.0 T=28.0

Figure 7: Velocity and Pressure field of Case B

It is of interest to note that in case B, more mass than in case A is gathered at the periphery of the spreading lamella. This is due to the larger dynamic contact angle, which causes a larger mean curvature at the periphery of the droplet. As a result, the velocity of lamella during receding, because of surface tension, is greater in case B, than in case A.

From the study of both cases, it is deduced that the greater the value of the advancing angle is, the greater the curvature of the spreading lamella is (moving outwards radically). As a result, the wetting forces due to surface tension are greater and delay the outward spreading of lamella. During the receding phase, the greater wetting forces in case B, accelerate the receding phase, the induced velocity field in the upper region of lamella is stronger and under the simultaneous effect of gravity the droplet vibrates more, before it reaches equilibrium.

6. Conclusions

The flow development arising from the normal impingement of a droplet onto a wall was numerically studied using a finite volume methodology with the Volume of Fluid (VOF) technique solving not only the liquid, but also the gas phase in contrast with other numerical methods. A higher order discretisation scheme was found imperative for the numerical solution of the transport equation for the VOF indicator in order to accurately track the droplet-wall interface. The results indicate that the evolution of the phenomenon in the early stages is not affected by the value of the advancing contact angle, but there is dependence between the value of dynamic contact angles and the velocity of the rim of the lamella, which affects the droplet spread and recoiling in latter stages. Generally, the use of VOF methodology is capable of predicting in a good way a two phase flow, getting

important information about the physics of such phenomena that experiment is not able to supply at the moment.

Acknowledgments: The financial support of the EU under contract N^{o} ENK6-2000-00051, 4th European Commission (2001-2003) is acknowledged.

7. References

[1] Cossali G.E., Goghe A., Marengo M., 1997. Experiments in Fluids 22, p463-472.
[2] Rioboo R. 2001. These de doctorat de l universite Paris 6.
[3] Mundo C., Sommerfeld M. and Tropea C., 1995. Int.J.Multiphase Flow 21 151.
[4] Hirt, C.W. and Nichols, B.D., 1981. J.Comput.Phys., Vol.39, p.201-225.
[5] Papadakis G. and Bergeles G, 1995. Int.J.Num. Meth. Heat Fluid Flow, Vol. 5, pp.49-62.
[6] Patankar, S.V.,Spalding, D.B.,1972. Int.J.Heat MassTransfer 15, 1787.
[7] Rhie,C., Chow,W., 1983. AIAA J. 21, p 1525-1532.
[8] Ubbink Onno, 1997. Ph.D thesis, University of London/Imperial College.
[9] J.Fukai, Y.Shiba, T. Yamamoto and O.Miyatake-D.Poulikakos, C.M.Megaridis and Z.Zhao. 1995. Physics of Fluids 7, p 236-247
[10] Hoffman, R.L 1975. J. Colloid Interface Sci. 50 p228-241.
[11] Blake, in 'Wettability' (J.C. Berg, Ed.) Dekker, New York, 1, 1993.
[12] Marco Marengo 'Dynamical contact angle under non-stationary conditions: theoretical attempt'